J. Fluid Mech. (1966), *vol.* 26, *part* 3, *pp.* 437–457
Printed in Great Britain

On the instability of ventilated cavities

By L. C. WOODS
Mathematical Institute, Oxford University

(Received 1 October 1965 and in revised form 11 February 1966)

It has been found that ventilated cavities extending behind hydrofoils, plates, and other two-dimensional bodies, oscillate when the air supply rate is sufficient to reduce the cavitation number to about one-fifth of its natural value. As the rate increases further, higher modes of oscillation occur in which the cavity–water interface supports several waves that are convected downstream towards the wake, which, owing to a pinching-off action replacing the usual entrainment sink, consists of a sequence of large bubbles drifting downstream. A theory of such flows that allows both for the convected velocity fluctuations in the cavity, and for the transport of bubble volume down the wake, is given in this paper. Coupled with a rather simple phenomenological relation between the pressure fluctuations within the cavity and the departure of the pinched-off rear portion of the cavity—explained in terms of the action of the re-entrant jet—this theory successfully predicts the resonance frequencies obtained in experiments by Silberman & Song.

The theory also provides a solution of the more general problem of determining the fluctuations in the pressure distribution over the whole surface of the body, when it is in a prescribed unsteady motion along its axis of symmetry (the theory is confined to symmetrical bodies and flows). Thus the growth in drag due to a sudden increment in the upstream velocity can be predicted, and also the damping forces acting on the body when it is forced to oscillate at a given frequency. It is shown that in all cases the body is unstable.

One important feature of the mathematical model chosen is that it completely avoids the presence of a time-dependent sink at infinity—with its associated infinite pressures—by conserving total volume of wake and cavity in just the same way as vorticity is conserved in unsteady aerofoil theory.

1. Introduction

The cavity that forms behind a submerged body moving at speed through a liquid is continuously supplied with gas and vapour from the cavity walls, a mixture that leaves by entrainment in the turbulent foam and liquid usually found at the end of the cavity and introduced into it by a re-entrant jet (see figure 1). Bubbles of gas and vapour pass downstream in the wake and are quickly reabsorbed into the liquid, which of course is most commonly water. Despite some fluctuation in the re-entrant jet, under steady flow conditions this natural cavity is quite stable, having a constant shape and a constant cavity pressure p_c, approximately equal to the vapour pressure of the liquid. The most important

parameter descriptive of the flow is the cavitation number $\sigma \equiv (p_\infty - p_c)/\frac{1}{2}\rho U^2$, where p_∞ and U are the pressure and velocity in the undisturbed flow well upstream of the body and ρ is the liquid density, assumed to be constant. Cavities will not form unless σ is small enough, and they increase in length as σ is made smaller. Now, while σ can be controlled through p_∞ and U, in some experimental circumstances it is of greater convenience to alter p_c through the introduction of air or other gas into the cavity through the base of the body. This reduces σ, and a so-called ventilated cavity will result when the air supply rate Q is large enough to reduce σ to the cavitation point.

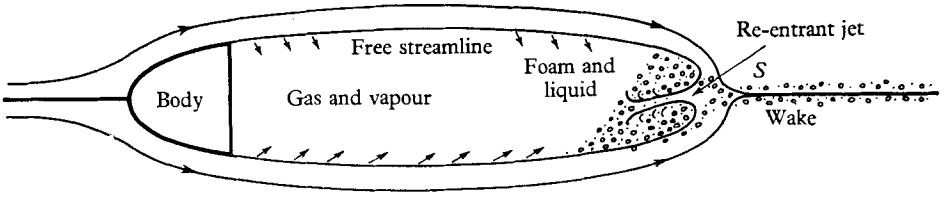

FIGURE 1. A natural cavity.

The relationship between Q, σ and σ_v—the natural cavitation number before cavitation—has been examined in an extensive set of experiments by Silberman & Song (1961), whose work has provided the stimulus for the present study. For two-dimensional cavities they arrive at an empirical law of the linear form $Q = a - b\sigma/\sigma_v$, provided $\sigma/\sigma_v \geqslant 0{\cdot}2$, and the corresponding cavities are quite stable. The only changes from natural cavitation are a substantial increase in the number of bubbles persisting in the wake, and some suppression of the re-entrant jet. However, for a critical value of σ/σ_v below 0·2 the ventilated cavity starts to vibrate violently, changing its length and width periodically, and the cavity pressure p_c oscillates about p_1, which denotes the mean value. The re-entrant jet is completely suppressed during that part of the cycle in which the cavity length is a maximum. Further increase in Q has no immediate effect on σ/σ_v; the oscillations become more violent, but their frequency remains constant. However, when a still higher value of Q is achieved, the cavity quickly increases in average length and pressure, and σ/σ_v suddenly drops. The new cavity vibrates less vigorously than the first, and its surface now carries a wave-form of two wavelengths that is convected downstream with the local stream velocity $q_1 = U(1+\sigma)^{\frac{1}{2}}$. Silberman & Song term this a two-stage cavity. Further increases in Q cause additional discontinuous changes in the average length L, the oscillation frequency ν, and in p_1 and σ/σ_v, and as many as six stages have been identified for flow past the two-dimensional normal plate. The nth stage supports n waves over the cavity length, moving downstream towards the cavity's closed end S at a speed of about q_1. Cavities of finite span are found to possess the same characteristics as described above for the two-dimensional types.

The key to the phenomenon just described lies in the way that vibrating cavities part with their cavity air. Steady entrainment no longer occurs, but is replaced by a fission process in which the last wave is periodically pinched off at a time when the cavity pressure is too low to sustain a cavity of greater than

average length. Figure 2 depicts four stages in a complete cycle for a three-stage cavity. Incidentally the time scale shown is related to real time t by $\tau = 2rUt/L$, where r is the ratio of the mean speed over the cavity, q_1, to the undisturbed speed U. Thus

$$r \equiv q_1/U = (1+\sigma)^{\frac{1}{2}}, \quad \sigma \equiv (p_\infty - p_1)/\tfrac{1}{2}\rho U^2. \tag{1}$$

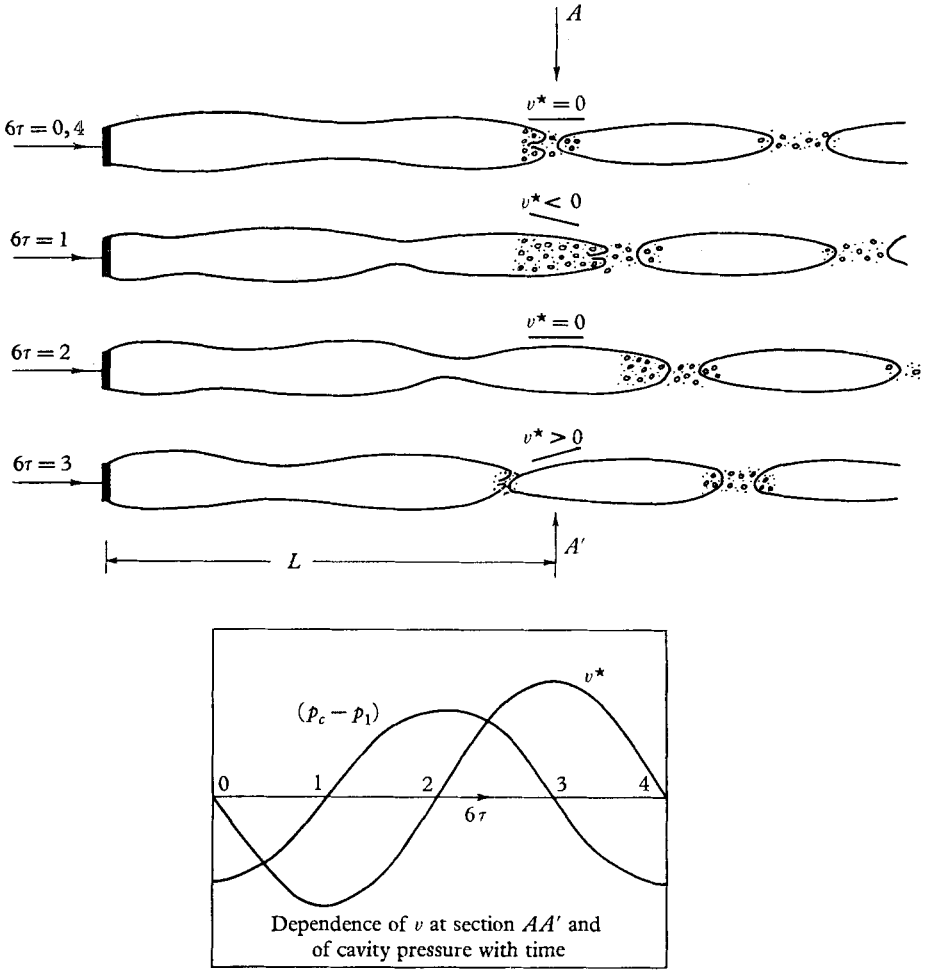

FIGURE 2. Evolution of a three-stage cavity.

The process shown in the figure is an idealization based on the description given by Silberman & Song. At $\tau = 0$, when the last wave is just pinched off, the re-entrant jet commences strongly, shooting water into the cavity at such a rate that the air supplied by the body together with this water is more than sufficient to keep pace with the expansion of the cavity caused by the convection downstream of the next wave. The result is that the cavity pressure increases steadily from the low value it achieved on the previous cycle to a maximum at $\tau = 2/6$, at which stage the re-entrant jet is considerably weakened and the air–water foam is being removed by entrainment just as in steady flow. Now the continuing lengthening of the cavity occurs with very little new water being added to it, so

that the pressure falls. This reduced pressure decrees a narrower and shorter cavity—a consequence of the usual steady-state theory—and this is achieved by a repetition of the pinching-off process. The cycle then repeats.

Also shown in figure 2 is the dependence on τ of v^*, the slope of the cavity surface at AA'. The lagging of $(p_c - p_1)$ behind v^* by 90° is an important experimental result, and supports the only phenomenological element we shall introduce into the theory. One final, and minor point is that, as shown in the figure, we have chosen as reference length L not the mean cavity length, but the shortest length in the cycle. The reason is that Silberman & Song found experimentally that the minimum length is closest to the length found for non-vibrating cavities at the same value of σ.

The theory we shall develop below aims not only at predicting the frequencies of vibration of the cavities, with the body held in a fixed position, but also at the solution of the more general problem of determining the fluctuations in the pressure over the surface of the body, when it itself is in a prescribed unsteady motion along its axis of symmetry. Thus, for example, we hope to be able to predict the growth of drag due to a sudden increment in the reference velocity U. Another question in which we are interested is the stability or not of oscillatory motions of the body; i.e. are there induced forces in phase with the velocity tending to augment the amplitude? The answers to these questions are given in §§ 7–9, but before this the physical model to be adopted and its mathematical consequences must be developed.

2. The physical model

An outline of the theory of the steady cavitating flow past a symmetrical body at zero incidence will be given in § 4, and the unsteady component of the flow will be treated as a linear perturbation on this basic steady flow. Thus the unsteady boundary conditions will be imposed at the surface of the body and the cavity as determined by the steady flow, but, as it will become clear, this will not mean that the cavity length must remain fixed during the perturbation.

Let θ denote the flow direction relative to the Ox-axis, the axis of symmetry of the flow; then in the steady flow the value of θ on the streamline $y = 0$ joining the rear of the cavity S to $x = \infty$, say v, will be zero; but in the unsteady flow v need not be zero (see figure 3). Certainly with vibrating ventilated cavities, it is clear from figure 2 that v will not vanish for a considerable distance downstream of S, whereas with natural cavities v will quickly decay to zero owing to the rapid re-absorption of the vapour from the host of small wake bubbles. The function $v(s)$, where s is distance measured along a streamline, is introduced to account for the *unsteady* component of the wake displacement thickness due to the convection of bubbles, large and small, downstream of S. While the underlying steady stream of bubbles will displace streamlines outwards, it will not contribute to v. One rather important restriction must be imposed on v, namely that the total volume of the cavity, plus the perturbation volume in the wake, must, at most, increase at a constant rate. This means that the source at infinity, required to accommodate the liquid displaced by the changing volume of cavity plus wake,

will be time independent, as required by the theorem analogous to Helmholtz's theorem on conservation of circulation (see Benjamin 1964 and Woods 1964 for a fuller discussion). Without this restriction the pressure at infinity is unbounded. Hence the flow depicted in figure 3 has a constant sink at infinity receiving the mean flux of volume convected by the bubbles, while the superimposed perturbation volume is positive or negative in a region according to whether there is a surplus or a deficiency in the wake bubbles in that region, and the *perturbation* in the *sum* of the wake and cavity volumes is zero. Now the waves, or other

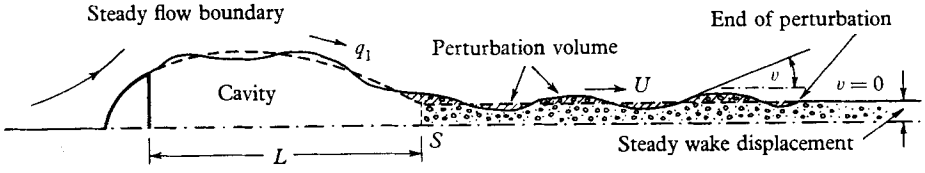

FIGURE 3. The physical model.

perturbations in the wake, may be assumed to be convected downstream with velocity U, unchanged in shape, apart from a possible decay in amplitude. Thus

$$v(s,t) = \exp[-\epsilon(s-s_1)]\, v(s_1, t-(s-s_1)/U), \tag{2}$$

s_1 being the value of s at the cavity end S.

In addition to the restriction on v imposed by the time independence of the sink at infinity, we could add the requirement that the waves on the cavity surface upstream of S are transmitted *smoothly* through S. However, as will be seen, this smooth-flow condition completely suppresses pressure fluctuations within the cavity, so that a singularity at S is required in a model for the resonance shown in figure 2.

In incompressible fluid dynamics the variable harmonic to θ is $\log q$, where q is the fluid speed. We shall write

$$\left.\begin{aligned} &\Omega \equiv \log(U/q), \quad \text{i.e. } q = U e^{-\Omega} \\ \text{and} \quad &\chi \equiv \Omega + i\theta = \log(U\,dz/dw), \quad \text{i.e. } U\,dz = e^{\chi}\,dw, \end{aligned}\right\} \tag{3}$$

where $w = \phi + i\psi$ is the complex stream function and $z = x + iy$. In (3) note that w, not z, is chosen as the independent variable, so, in accordance with the linearization mentioned above, w is the stream function of the mean steady flow, e.g. over the cavity surface

$$dw = d\phi = q_1\,ds = rU\,ds. \tag{4}$$

More convenient independent variables are defined by

$$\alpha \equiv \frac{w - \frac{1}{2}(\phi_S + \phi_C)}{\frac{1}{2}(\phi_S - \phi_C)}, \quad \alpha = \delta + i\beta, \quad \phi_S - \phi_C = q_1 L = rUL, \tag{5}$$

and

$$\alpha \equiv -\cos\zeta, \quad \zeta = \gamma + i\eta, \tag{6}$$

where ϕ_C and ϕ_S are the values of ϕ at the separation point C and the singularity S, and we have slightly modified the meaning of L as indicated in figure 4. The ζ plane, also shown in figure 4, places the body on $\gamma = 0$, $0 \leqslant \eta < \eta_0$, the wake on

$\gamma = \pm\pi$, $0 \leqslant \eta < \infty$, and the cavity surface on $\eta = 0$, $-\pi \leqslant \gamma \leqslant \pi$. Its merit will become clear later.

The pressure p is given by

$$p + \tfrac{1}{2}\rho q^2 + \int_{-\infty}^{s} \frac{\partial q}{\partial t}\, ds = p_0 + \tfrac{1}{2}\rho q_0^2 = p_\infty + \tfrac{1}{2}\rho U^2, \tag{7}$$

the subscript '0' denoting steady values. (Steady, *constant* values over the cavity like p_1 and q_1 will not have this subscript added.) In (7) we have integrated along

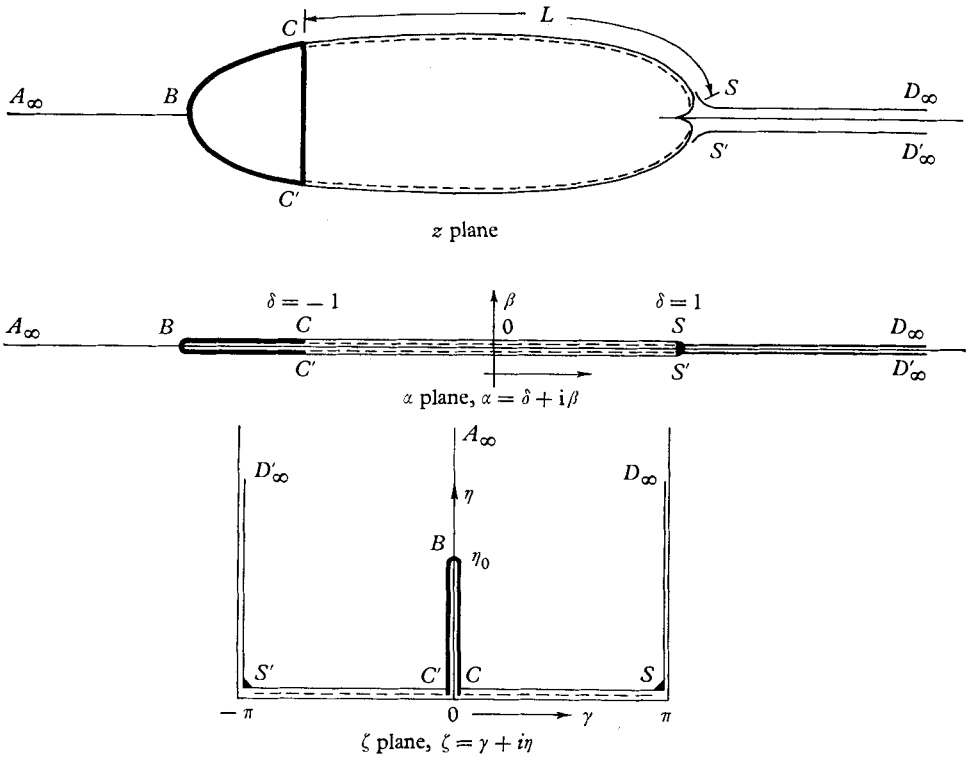

FIGURE 4. Independent variables.

$\psi = 0$ from $\phi = -\infty$. In the cavity the pressure p_c will be constant at any instant of time, sound waves through the vapour being instantaneously transmitted on the hydrodynamic time-scale, thus, by (3), (4), (5) and (7) and some obvious linearizations,

$$\frac{\partial \Gamma_c}{\partial \xi} + \frac{\partial \Gamma_c}{\partial \tau} = 0, \quad \Gamma_c \equiv (\Omega_c - \Omega_1), \quad \text{on} \quad \beta = 0, \quad -1 \leqslant \xi \leqslant 1, \tag{8}$$

where ξ is a particular value of δ,

$$\tau \equiv (2rU/L)t \tag{9}$$

is a 'reduced' time scale for the cavity disturbance, supposed to be initiated at $t = 0$, and where $\Omega_c = \log(U/q_c)$, $\Omega_1 = \log(U/q_1)$ so that $\Gamma_c \approx (q_1 - q_c)/q_1$. It has been assumed here that U is independent of time—the gust problem mentioned

in the last paragraph of § 1 can be simulated by impulsive motions of the body itself. On integrating (8) we get

$$\Gamma_c(\xi,\tau) = \begin{cases} \Gamma_c(-1,\tau-\xi-1) = \Gamma_c(-1,\sigma) & (|\xi|<1,\ 0<\sigma), \\ 0 & (\text{otherwise}), \end{cases} \tag{10}$$

where $\sigma \equiv \tau - \xi - 1$, and (2) can be put into a similar form, viz.

$$v(\xi,\hat{\tau}) = \begin{cases} \exp[-\epsilon(\xi-1)]\, v(1,\hat{\tau}-\xi+1) = \exp[-(\hat{\tau}-\hat{\sigma})]\, v(1,\hat{\sigma}) & (1<\xi,\ 0<\hat{\sigma}) \\ 0 & (\text{otherwise}), \end{cases} \tag{11}$$

where

$$\hat{\tau} \equiv \tau/r^2, \quad \hat{\sigma} \equiv \hat{\tau} - \xi + 1,$$

and the damping length $1/\epsilon$ has been non-dimensionalized. Figure 5 illustrates equations (10) and (11).

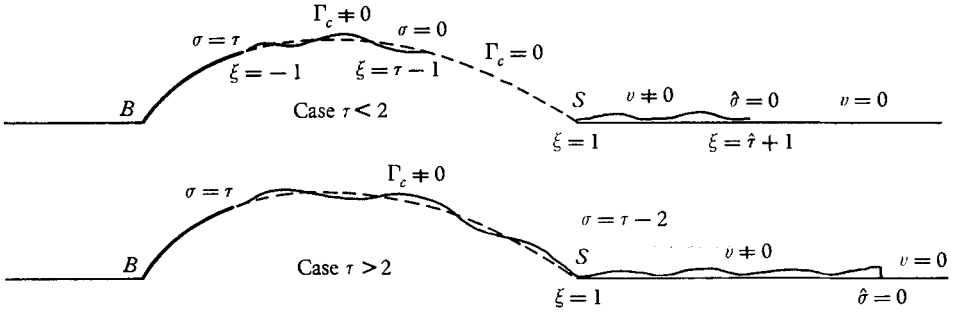

FIGURE 5. Convection of the perturbations.

On the body the boundary condition can be expressed as a prescribed direction of flow, viz.

$$\theta(\xi,\tau) = \begin{cases} \theta_0(\xi) + \theta_2(\xi,\tau) & (\xi_0 \leqslant \xi \leqslant -1), \\ 0 & (-\infty \leqslant \xi \leqslant \xi_0), \end{cases} \tag{12}$$

where the perturbation θ_2 is related to the small unsteady velocity of the surface normal to itself, say v, by $\theta_2 = v/q_0$ (see figure 6). For a rigid body the only motion allowed by the restriction of symmetry about $y = 0$ is motion along this axis; suppose the perturbation velocity is $u(t)$, then $v = -u \sin\theta_0$ and

$$\theta_2 = -u(t)\,(\sin\theta_0)/q_0. \tag{13}$$

For a sudden gust of magnitude V convected on to the body with velocity U we take

$$u(t) = -V\mathbf{U}(t), \tag{14}$$

where $\mathbf{U}(t)$ is the unit function. The simplest non-rigid motion that can be considered requires a hinge at the front stagnation point B (see figure 7). Suppose the body is a wedge of small angle $\theta_0 + \theta_u(t)$, then one can use the linearization

$$\theta_2 = a\theta_u'(t)/q_0 \approx \theta_u'(t)\,(rL/2U)\,(\xi - \xi_0), \tag{15}$$

on replacing ϕ by Us in (5); a and ξ are defined in figure 7.

Our mixed boundary-value problem is thus:

$$\text{On} \quad \beta = 0, \begin{cases} \theta(\xi,\tau) = \theta_0(\xi) + \theta_2(\xi,\tau) & (-\infty < \xi < -1), \\ \Omega(\xi,\tau) = \Omega_1 + \Gamma_c(\xi,\tau) & (-1 < \xi < 1), \\ \theta(\xi,\hat{\tau}) = \upsilon(\xi,\hat{\tau}) & (1 < \xi < \infty), \end{cases} \tag{16}$$

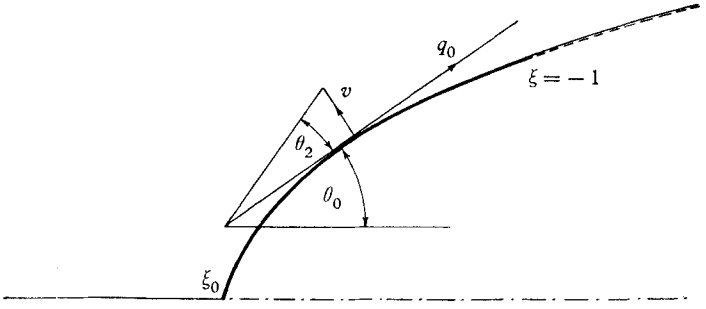

FIGURE 6. Boundary condition on the body.

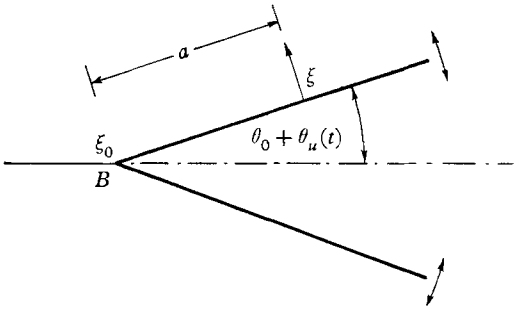

FIGURE 7. Hinged wedge.

where $\theta_0(\xi)$ and $\theta_2(\xi,\tau)$ are prescribed functions, Ω_1 is a given constant, viz.

$$\Omega_1 = \Omega_{c0} = -\tfrac{1}{2}\log(1+\sigma), \tag{17}$$

and Γ_c and υ satisfy (10) and (11). In addition we have the conditions near infinity

$$\lim_{\alpha\to\infty} \chi(\alpha) = 0, \tag{18}$$

$$\lim_{\alpha\to\infty} \alpha\chi(\alpha) = -M, \tag{19}$$

where M is a constant. The first of these follows immediately from (3) and the chosen values $q_\infty = U$, $\theta_\infty = 0$, while the second is easily verified to be the restriction on the nature of the sink at infinity—if $M = 0$ the sink for the steady component of flow also vanishes, and the cavity is closed.

Returning to the point made at the end of the first paragraph of this section, we note that, while S is a fixed point, the cavity length is free to change by the introduction of υ (cf. figure 3). Of course, if there are no bubbles in the wake, υ will be localized near $\xi = 1$, and in this case its effect can be incorporated in a singularity at S as described later. The point S is simply the point chosen to mark the change from one type of boundary condition to the other.

3. The solution to the boundary-value problem

We now seek a complex function $\chi(\alpha)$ satisfying (16) on $\beta = 0$. As a first step we can write down (see p. 148 of Woods 1961)

$$\chi(\alpha,\tau) = \frac{1}{\pi}\left(\frac{\alpha+1}{\alpha-1}\right)^{\frac{1}{2}}\left\{\left(\int_{-\infty}^{-1}+\int_{1}^{\infty}\right)\theta_s\left(\frac{\xi-1}{\xi+1}\right)^{\frac{1}{2}}\frac{d\xi}{\xi-\alpha}+\int_{-1}^{1}\Omega_s\left(\frac{1-\xi}{1+\xi}\right)^{\frac{1}{2}}\frac{d\xi}{\xi-\alpha}\right\}, \tag{20}$$

where θ_s and Ω_s denote values on $\beta = 0$, and are functions of ξ and τ. Equation (18) is satisfied by (20), while (19) requires that

$$\frac{1}{\pi}\left(\int_{-\infty}^{-1}+\int_{1}^{\infty}\right)\theta_s\left(\frac{\xi-1}{\xi+1}\right)^{\frac{1}{2}}d\xi+\frac{1}{\pi}\int_{-1}^{1}\Omega_s\left(\frac{1-\xi}{1+\xi}\right)^{\frac{1}{2}}d\xi - M = 0.$$

Bearing in mind that $(\xi^2-1)^{\frac{1}{2}}$ takes the values $\sqrt{(\xi^2-1)}$, $i\sqrt{(1-\xi^2)}$ and $-\sqrt{(\xi^2-1)}$ on $1 < \xi < \infty$, $-1 < \xi < 1$, and $-\infty < \xi < -1$ respectively, we may write (20) in the alternative forms

$$\chi(\alpha,\tau) = -\frac{(\alpha^2-1)^{\frac{1}{2}}}{\pi}\left\{\int_{-\infty}^{-1}\frac{\theta_s\,d\xi}{(\xi-\alpha)\sqrt{(\xi^2-1)}}+\int_{-1}^{1}\frac{\Omega_s\,d\xi}{(\xi-\alpha)\sqrt{(1-\xi^2)}} - \int_{1}^{\infty}\frac{\theta_s\,d\xi}{(\xi-\alpha)\sqrt{(\xi^2-1)}}\right\} - \mathscr{S}\left(\frac{\alpha+1}{\alpha-1}\right)^{\frac{1}{2}}, \tag{21}$$

$$\chi(\alpha,\tau) = -\frac{(\alpha^2-1))^{-\frac{1}{2}}}{\pi}\left\{\int_{-\infty}^{-1}\frac{\theta_s\sqrt{(\xi^2-1)}}{\xi-\alpha}d\xi-\int_{-1}^{1}\frac{\Omega_s\sqrt{(1-\xi^2)}}{\xi-\alpha}d\xi - \int_{1}^{\infty}\frac{\theta_s\sqrt{(\xi^2-1)}}{\xi-\alpha}d\xi\right\}, \tag{22}$$

where

$$\mathscr{S} \equiv \frac{1}{\pi}\int_{-\infty}^{-1}\frac{\theta_s\,d\xi}{\sqrt{(\xi^2-1)}}+\frac{1}{\pi}\int_{-1}^{1}\frac{\Omega_s\,d\xi}{\sqrt{(1-\xi^2)}}-\frac{1}{\pi}\int_{1}^{\infty}\frac{\theta_s\,d\xi}{\sqrt{(\xi^2-1)}}. \tag{23}$$

It is also convenient to rewrite the equation containing M as

$$M = -\frac{1}{\pi}\int_{-\infty}^{-1}\frac{\theta_s(\xi-1)\,d\xi}{\sqrt{(\xi^2-1)}}-\frac{1}{\pi}\int_{-1}^{1}\frac{\Omega_s(\xi-1)\,d\xi}{\sqrt{(1-\xi^2)}}+\frac{1}{\pi}\int_{1}^{\infty}\frac{\theta_s(\xi-1)\,d\xi}{\sqrt{(\xi^2-1)}}. \tag{24}$$

Equation (21) shows that, unless $\mathscr{S}$ is zero, there is a singularity at $\alpha = 1$, the rear end of the cavity. However, we shall not put $\mathscr{S}$ equal to zero at this stage, for to do so would be losing a vital degree of freedom in our solution. Alternatively, we could put $\mathscr{S} = 0$, and re-introduce a single degree of freedom by making either Ω_s or θ_s large near $\xi = 1$, but the outcome will be equations of the same form as (21) to (24). For example, with $\mathscr{S}$ zero in (21) and (23) and with θ_s replaced by $v+v^*\{\mathbf{U}(\xi-1)-\mathbf{U}(\xi-1-\epsilon)\}$, $\epsilon \ll 1$, where $\mathbf{U}(\xi)$ is the unit function, the choice $v^* = -\pi\sqrt{(2\epsilon)}\mathscr{S}$, returns one to the present forms of (21) to (24) (to the lowest order in ϵ) except that in $(1,\infty)$ θ_s is now v. This provides the physical interpretation of $\mathscr{S}$ shown in figure 8.

In the ζ plane defined by (6) and drawn in figure 4, (21), (23) and (24) take the neater forms

$$\chi(\zeta,\tau) = \frac{i\sin\zeta}{\pi}\left\{\int_0^\infty \left(\frac{\theta_s}{\cosh\eta'-\cos\zeta}+\frac{v}{\cosh\eta'+\cos\zeta}\right)d\eta' + \int_0^\pi \frac{\Omega_s d\gamma'}{\cos\gamma'-\cos\zeta}\right\} + i\mathscr{S}\tan\tfrac{1}{2}\zeta, \tag{25}$$

$$\mathscr{S} = \frac{1}{\pi}\int_0^\infty (\theta_s - v)\,d\eta' + \frac{1}{\pi}\int_0^\pi \Omega_s\,d\gamma', \tag{26}$$

$$M = \mathscr{S} + \frac{1}{\pi}\int_0^\infty (\theta_s - v)\cosh\eta'\,d\eta' + \frac{1}{\pi}\int_0^\pi \Omega_s\cos\gamma'\,d\gamma', \tag{27}$$

where now θ_s is the boundary value of θ over $-\infty < \xi < -1$, and v refers, as usual, to the wake, $1 < \xi < \infty$. In these equations η' and γ' are running variables on $\gamma = 0$ and $\eta = 0$, respectively, and ζ is a general point in the plane.

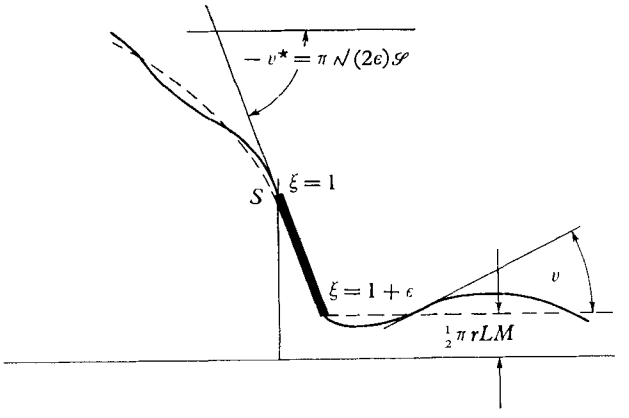

FIGURE 8. The singularity at S.

The point at infinity in the z plane is at $\eta = \infty$, and in this neighbourhood (25) has the expansion

$$\chi = 2M e^{i\zeta} + 2N e^{2i\zeta} + O(e^{3i\zeta}), \tag{28}$$

where

$$N \equiv \frac{1}{\pi}\int_0^\infty (\theta_s - v)\cosh 2\eta'\,d\eta' + \frac{1}{\pi}\int_0^\pi \Omega_s\cos 2\gamma'\,d\gamma' - \mathscr{S}. \tag{29}$$

Now by (3), (5) and (6), near infinity,

$$z = \frac{1}{U}\int e^{\chi}dw = \tfrac{1}{2}rL\int (1 + 2M e^{i\zeta} + 2(M^2+N)e^{2i\zeta} + \ldots)\sin\zeta\,d\zeta,$$

as

$$dw = \tfrac{1}{2}rUL\,d\alpha = \tfrac{1}{2}rUL\sin\zeta\,d\zeta. \tag{30}$$

Hence

$$z \sim \tfrac{1}{2}rL\{-\tfrac{1}{2}e^{-i\zeta} + iM\zeta + C + (M^2+N-\tfrac{1}{2})e^{i\zeta} + \ldots\}, \tag{31}$$

where C is a real constant of integration. Notice that the imaginary part of z jumps from zero to $\frac{1}{2}\pi rLM$ as one moves from A_∞ at $\eta = \infty$, $\gamma = 0$, to D_∞ at $\eta = \infty$, $\gamma = \pi$; thus the width of the steady wake is

$$y_0 = \tfrac{1}{2}\pi rLM, \tag{32}$$

as marked on figure 8.

At this stage it is convenient to separate the equations into their steady and unsteady components, and for this purpose an outline of the theory of steady cavitating flow is given in the next section.

4. Steady cavitating flow

The results will be expressed in terms of the variable ζ, with some gain in simplicity. By (16), in steady flow (25) to (27) give

$$\chi_0(\zeta) = \Omega_1 + \frac{i\sin\zeta}{\pi}\int_0^{\eta_0} \frac{\theta_0 d\eta'}{\cosh\eta' - \cos\zeta} + i\mathscr{S}_0 \tan\tfrac{1}{2}\zeta, \tag{33}$$

$$\mathscr{S}_0 = \Omega_1 + \frac{1}{\pi}\int_0^{\eta_0} \theta_0 d\eta, \tag{34}$$

$$M = \mathscr{S}_0 + \frac{1}{\pi}\int_0^{\eta_0} \theta_0 \cosh\eta\, d\eta, \tag{35}$$

where η_0 is the value of η at the front stagnation point B, corresponding to ξ_0. By (5)

$$\tfrac{1}{2}L(\xi_0+1) = (\phi_C - \phi_B)/q_1 = l, \tag{36}$$

say, where for slender bodies the distance l is approximately equal to the length of the wetted surface from B to C. Then with

$$m^2 \equiv l/(l+L), \tag{37}$$

a measure of the ratio of this characteristic body dimension to a distance approximately equal to the whole length of wetted and cavity surface, we have

$$\frac{l}{L} = \frac{m^2}{1-m^2}, \quad \eta_0 = \log\left(\frac{1+m}{1-m}\right), \quad \sinh\eta_0 = \frac{2m}{1-m^2}, \tag{38}$$

which will be needed shortly.

The drag coefficient based on a characteristic length c is

$$C_D = -\frac{2i}{c\rho U^2}\int_{\mathscr{C}_0} (p - p_1)\, dz, \tag{39}$$

where $\mathscr{C}_0$ is the whole of the wetted surface of the body. In steady flow it follows from (1), (3), (7) and (30) that

$$C_{D0} = -\frac{i}{2}\frac{L}{c}r^2\left\{\int_{\mathscr{C}_0} \exp(\chi_0 - \Omega_1)\, d\alpha - \int_{\mathscr{C}_0} \exp[-(\overline{\chi_0 - \Omega_1})]\, d\bar{\alpha}\right\}, \tag{40}$$

on taking advantage of the fact that $d\alpha = d\bar{\alpha}$ on the profile. In the ζ plane, $Re(\chi_0 - \Omega_1) = 0$ on the real axis, and consequently χ_0 can be continued analytically to the lower half plane by $\chi_0(\bar{\zeta}) = -\overline{\chi_0(\zeta)} + 2\Omega_1$, then the second integral in (40) can be taken to be the integral of $\exp(\chi_0 - \Omega_1)(d\alpha/d\zeta)$ along the conjugate contour to $\mathscr{C}_0$ in the lower half plane (see figure 9). Then with $\mathscr{C} = \mathscr{C}_0 + \overline{\mathscr{C}}_0$, (40) becomes

$$C_{D0} = -\frac{i}{2}\frac{L}{c}r^2\int_{\mathscr{C}} \exp(\chi_0 - \Omega_1)\sin\zeta\, d\zeta.$$

Clearly $\mathscr{C}$ can now be deformed into the large contour shown in figure 9. From the expansion (28) near $\mathscr{C}_\infty$, and its analytic continuation to $\overline{\mathscr{C}}_\infty$, we find that like

the contributions from $\mathscr{C}_\pi$ and $\mathscr{C}'_\pi$, the contributions from $\mathscr{C}_\infty$ and $\overline{\mathscr{C}}_\infty$ cancel. We are left with a single closed loop about S. At $\zeta = \pi + z$, we find

$$\chi_0 - \Omega_1 = -2i\mathscr{S}_0 z + izb_0 + O(z^3), \tag{41}$$

where

$$b_0 \equiv \tfrac{1}{6}\mathscr{S}_0 - \frac{1}{\pi}\int_0^\infty \frac{\theta_0\, d\eta}{1+\cosh\eta}.$$

Thus $\exp(\chi_0 - \Omega_1)\sin\zeta\, d\zeta = \exp(-2i\mathscr{S}_0/z)\{-z - ib_0 z^2 + (\frac{1}{2}b_0^2 + \frac{1}{6})z^3 + \ldots\}dz$,

and as $\int \exp(-2i\mathscr{S}_0/z)\, z^{n-1}\, dz = 2\pi i(-2i\mathscr{S}_0)^n/n$ for a loop enclosing S, we get

$$C_{D0} = 2\pi r^2(L/c)\mathscr{S}_0^2\{1 + \tfrac{2}{3}b_0\mathscr{S}_0 + \tfrac{1}{6}(b_0^2 + \tfrac{1}{3})\mathscr{S}_0^2 + \ldots\}. \tag{42}$$

There is little point in expanding further because the relation between l and the actual wetted length, c say, while near unity for slender bodies, is not easy to

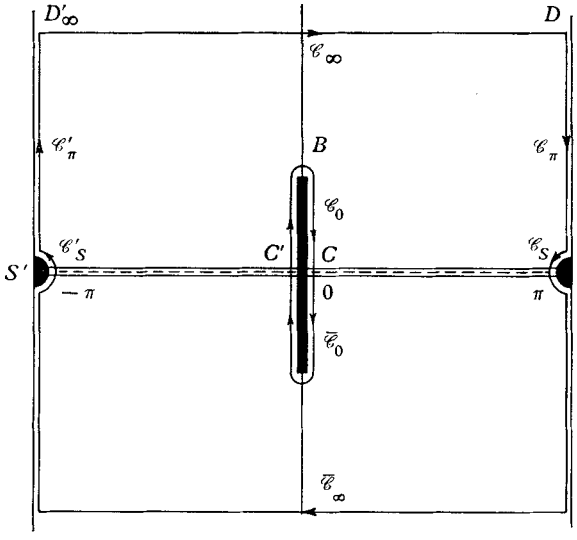

FIGURE 9. Contour for drag coefficient.

determine for bluff bodies. For the normal plate, $l \approx 2c/(4+\pi)$ (see p. 446 of Woods 1961).

In steady flow the coefficient N defined in (29) is

$$N_0 = \frac{1}{\pi}\int_0^\infty \theta_0(\cosh 2\eta + \cosh\eta)\, d\eta, \tag{43}$$

provided $M = 0$. In this case we can show that N_0 is closely related to the cavity volume V_0. Let C be the contour enclosing the body, the cavity and the singularity S; then

$$V_0 = \tfrac{1}{2}\operatorname{Im}\int_C z\, d\bar{z} = \frac{1}{2U}\operatorname{Im}\int_C z\, e^{\bar{\chi}_0}\, dw = \frac{1}{2Ur^2}\operatorname{Im}\int_C z\, e^{-\chi_0}\, dw + V_b,$$

where

$$V_b = \frac{1}{2U}\operatorname{Im}\int_{\mathscr{C}_0} z\left(1 - \left(\frac{q_0}{q_1}\right)^2\right) d\bar{z}$$

is a volume rather smaller than that of the body alone that we shall ignore.

Now we can replace C by $\mathscr{C}_\infty$ (see figure 9), and make use of (28) and (31), plus the restriction $M = 0$, to find

$$V_0 = \tfrac{1}{4}\pi L^2 N_0 \tag{44}$$

as an approximation to the volume.

With very long cavities m is small and $\eta_0 \approx 2m$. Then, defining an average body slope by

$$\theta_a \equiv \frac{1}{\eta_0}\int_0^{\eta_0} \theta_0 \, d\eta, \tag{45}$$

we find to first order in m that (34), (35), (42) and (44) reduce to

$$2\mathscr{S}_0 = -\sigma + \frac{4m\theta_a}{\pi}, \quad M = \mathscr{S}_0 + \frac{2m\theta_a}{\pi}, \quad C_{D0} = \frac{l}{c}\frac{8}{\pi}(1+\sigma)\theta_a^2, \tag{46}$$

and

$$V_0 = mL^2\theta_a \quad (M = 0). \tag{47}$$

It is interesting to note that the singularity $\mathscr{S}_0$ can be eliminated by introducing a sting of width $2y_0 = \pi r L M \approx 2r\theta_a l/m$ into the rear of the cavity, and that this halves the cavitation number for a given cavity length.

5. The pressure and drag in unsteady flow

At a point ξ on the wetted surface, the linear perturbation form of (7) gives

$$p(\xi,\tau) - p_0(\xi) = \rho q_0^2(\xi)\, F(\xi,\tau), \tag{48}$$

where

$$F \equiv \Gamma + \int_{-\infty}^{\xi} \dot{\Gamma}\, d\xi, \quad F \equiv \Omega - \Omega_0 \tag{49}$$

and the dot denotes the derivative with respect to τ. At a point α on the real axis in $(-\infty, -1)$, it follows from (16) and (22) that

$$\Gamma(\alpha,\tau) = \frac{1}{\pi\sqrt{(\alpha^2-1)}}\left\{\int_{-\infty}^{-1}\frac{\theta_2\sqrt{(\xi^2-1)}}{\xi-\alpha}\,d\xi - \int_{-1}^{1}\frac{\Gamma_c\sqrt{(1-\xi^2)}}{\xi-\alpha}\,d\xi - \int_1^{\infty}\frac{v\sqrt{(\xi^2-1)}}{\xi-\alpha}\,d\xi\right\}, \tag{50}$$

and a corresponding result can be written down from (21). Integration of each term in (50) by parts, differentiation with respect to τ, integration with respect to α, and finally the addition of the result to the formula for Γ derived from (21) leads to

$$F = \frac{1}{\pi}\int_{-\infty}^{-1}(\theta_2+\Theta)\,G(\xi,\alpha)\,d\xi - I - \frac{1}{\pi}\int_1^{\infty}\left\{v + \int_1^{\xi}\dot{v}\,d\xi\right\}G(\xi,\alpha)\,d\xi + \delta\left\{1 - \left(\frac{\alpha+1}{\alpha-1}\right)^{\frac{1}{2}}\right\}, \tag{51}$$

where

$$\Theta \equiv \int_{-\infty}^{\xi}\dot{\theta}_2(\xi,\tau)\,d\xi, \tag{52}$$

$$G \equiv \left\{\frac{\sqrt{(\alpha^2-1)}}{\xi-\alpha} - 1\right\}\frac{1}{\sqrt{(\xi^2-1)}} = -\left\{1 + \frac{(\alpha^2-1)^{\frac{1}{2}}}{\xi-\alpha}\right\}, \tag{53}$$

$\delta \equiv \mathscr{S} - \mathscr{S}_0$ and I has $G'\left(\Gamma_c + \int_1^{\xi}\dot{\Gamma}_c\,d\xi\right)$ for its integrand, where G' is like G except

that (ξ^2-1) is replaced by $(1-\xi^2)$. As $\int_{-1}^{1} G'\,d\xi = 0$, it follows from (8) that $I = 0$. Differentiating (11) we find $r^2\dot{v} = -\epsilon v - \partial v/\partial\xi$, hence

$$v + \int_1^{\xi} \dot{v}\,d\xi = v - \Psi + \text{const.},$$

where

$$\Psi \equiv \frac{1}{r^2}\left\{v + \epsilon\int_1^{\xi} v\,d\xi\right\}, \tag{54}$$

and (51) can be written

$$F = \frac{1}{\pi}\int_{-\infty}^{-1} (\theta_2+\Theta)\,G(\xi,\alpha)\,d\xi - \frac{1}{\pi}\int_1^{\infty} (v-\Psi)\,G(\xi,\alpha)\,d\xi + \delta\left\{1-\left(\frac{\alpha+1}{\alpha-1}\right)^{\frac{1}{2}}\right\}. \tag{55}$$

At $\alpha = -1$, $F = F^*$ say, and (48) and (55) give the cavity pressure fluctuations:

$$\frac{p_c-p_1}{\rho q_1^2} \equiv F^* = \delta - \frac{1}{\pi}\int_{-\infty}^{-1} \frac{\theta_2+\Theta}{\sqrt{(\xi^2-1)}}\,d\xi + \frac{1}{\pi}\int_1^{\infty} \frac{v-\Psi}{\sqrt{(\xi^2-1)}}\,d\xi. \tag{56}$$

By (3), (6), (39) and (48) the unsteady component of the drag coefficient is

$$C_D - C_{D0} = \frac{2i}{c\rho U^2}\int_{\mathscr{C}_0} (p-p_0)\,d\bar{z} = i\frac{Lr}{c}\int_{\mathscr{C}_0} F\,e^{-\chi_0}\sin\zeta\,d\zeta,$$

where F can be written as an analytic function of ζ by putting

$$G = -\left\{1+\frac{i\sin\zeta}{\xi+\cos\zeta}\right\}\frac{1}{\sqrt{(\xi^2-1)}} \quad \text{and} \quad 1-\left(\frac{\alpha+1}{\alpha-1}\right)^{\frac{1}{2}} = 1+i\tan\tfrac{1}{2}\zeta,$$

in (56). The contour $\mathscr{C}_0$ can now be replaced by $\mathscr{C}'_S+\mathscr{C}_\infty+\mathscr{C}_S$ as defined in figure 10, the contributions from the real axis and from $\mathscr{C}'_\pi+\mathscr{C}_\pi$ being zero. Near $\zeta = \pi$ it follows from (41) and (55) that

$$\frac{1}{r}F\,e^{-\chi_0}\sin\zeta\,d\zeta = \exp(2i\mathscr{S}_0/z)\{\beta_0+\beta_1 z+O(z^2)\}\,dz,$$

β_0, β_1 being constants, and, provided $\mathscr{S}_0 \leqslant 0$, the contour integral of this quantity about the indentations $\mathscr{C}_S$ and $\mathscr{C}'_S$—both in the *upper* half-plane—vanishes in the limit as the radii of the indentations tend to zero. That $\mathscr{S}_0$ is very unlikely to be positive in a practical case can be seen from the second equation of (46). From an equation like (28) for χ_0 and (55) we easily evaluate the contribution from $\mathscr{C}_\infty$, and so find the result

$$C_D - C_{D0} = 2\pi\frac{L}{c}r\left\{\frac{1}{\pi}\int_{-\infty}^{-1}\frac{\theta_2+\Theta}{\sqrt{(\xi^2-1)}}\,\xi\,d\xi - \frac{1}{\pi}\int_1^{\infty}\frac{v-\Psi}{\sqrt{(\xi^2-1)}}\,\xi\,d\xi - \delta\right\}, \tag{57}$$

where by (16) and (23)

$$\delta = \frac{1}{\pi}\int_{-\infty}^{-1}\frac{\theta_2\,d\xi}{\sqrt{(\xi^2-1)}} + \frac{1}{\pi}\int_{-1}^{1}\frac{\Gamma_c\,d\xi}{\sqrt{(1-\xi^2)}} - \frac{1}{\pi}\int_1^{\infty}\frac{v\,d\xi}{\sqrt{(\xi^2-1)}}. \tag{58}$$

Similarly, from (24) and the fact that M is constant, we have

$$0 = \frac{1}{\pi}\int_{-\infty}^{-1}\frac{\theta_2(\xi-1)}{\sqrt{(\xi^2-1)}}\,d\xi + \frac{1}{\pi}\int_{-1}^{1}\frac{\Gamma_c(\xi-1)}{\sqrt{(1-\xi^2)}}\,d\xi - \frac{1}{\pi}\int_1^{\infty}\frac{v(\xi-1)}{\sqrt{(\xi^2-1)}}\,d\xi, \tag{59}$$

and on combining (57) to (59) we find the alternative form

$$C_D - C_{D0} = 2\frac{L}{c} r \left\{ \int_{-\infty}^{-1} \frac{\Theta}{\sqrt{(\xi^2-1)}} \xi\, d\xi + \int_1^{\infty} \frac{\Psi}{\sqrt{(\xi^2-1)}} \xi\, d\xi - \int_{-1}^{1} \frac{\Gamma_c}{\sqrt{(1-\xi^2)}} \xi\, d\xi \right\}. \tag{60}$$

It remains to calculate expressions for v and Γ_c from the pair of integral equations (58) and (59), plus some hypothesis from which the value of δ can be found.

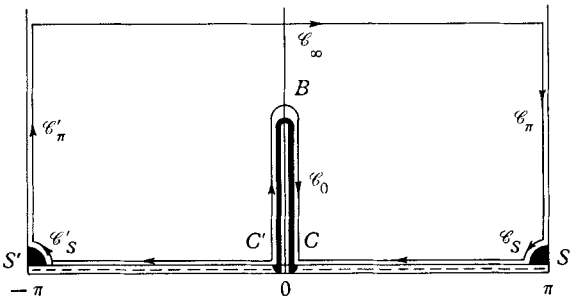

FIGURE 10. Contour for unsteady component of drag coefficient.

6. Solution of the integral equations for Γ_c and v

Let

$$a_0 \equiv \frac{1}{\pi}\int_{-\infty}^{-1} \frac{\theta_2\, d\xi}{\sqrt{(\xi^2-1)}}, \quad a_1 \equiv \frac{-1}{\pi}\int_{-\infty}^{-1} \frac{\theta_2 \xi\, d\xi}{\sqrt{(\xi^2-1)}}, \tag{61}$$

then by (10), (11), (58) and (59) can be written in the forms

$$\delta - a_0 = \frac{1}{\pi}\int_{-\infty}^{\infty} \{\Gamma_c(-1,\sigma)\,\mathbf{U}(\sigma)\} \left\{ \frac{\mathbf{U}(1-\{\tau-\sigma-1\}^2)}{\sqrt{(1-\{\tau-\sigma-1\}^2)}} \right\} d\sigma$$
$$- \frac{1}{\pi}\int_{-\infty}^{\infty} \{v(1,\hat{\sigma})\,\mathbf{U}(\hat{\sigma})\} \left\{ \frac{\mathbf{U}(\hat{\tau}-\hat{\sigma})\, e^{-\epsilon(\hat{\tau}-\hat{\sigma})}}{\sqrt{(\{\hat{\tau}-\hat{\sigma}+1\}^2-1)}} \right\} d\hat{\sigma},$$

$$a_0 + a_1 = \frac{1}{\pi}\int_{-\infty}^{\infty} \{\Gamma_c(-1,\sigma)\,\mathbf{U}(\sigma)\} \left\{ \mathbf{U}(1-\{\tau-\sigma-1\}^2)\, \frac{(\tau-\sigma-1)}{\sqrt{(1-\{\tau-\sigma-1\}^2)}} \right\} d\sigma$$
$$- \frac{1}{\pi}\int_{-\infty}^{\infty} \{v(1,\hat{\sigma})\,\mathbf{U}(\hat{\sigma})\} \left\{ \mathbf{U}(\hat{\tau}-\hat{\sigma})\, \frac{(\hat{\tau}-\hat{\sigma})\, e^{-\epsilon(\hat{\tau}-\hat{\sigma})}}{\sqrt{(\{\hat{\tau}-\hat{\sigma}+1\}^2-1)}} \right\} d\hat{\sigma},$$

on making use of unit functions to cope with the inequalities in (10) and (11). Let v^* and Γ_c^* denote the functions $\mathbf{U}(x)\,v(1,x)$ and $\mathbf{U}(x)\,\Gamma_c(-1,x)$, and denote the two-sided Laplace transform of v^* and Γ_c^* by $\mathscr{L}(v^*)$ and $\mathscr{L}(\Gamma_c^*)$; then, on making use of some results given by van der Pol & Bremmer (1950), we can transform these equations with respect to τ to find

$$\mathscr{L}(\Gamma_c^*)\, e^{-p} I_0(p) - (r^2/\pi)\, \mathscr{L}(v^*)\, e^{\hat{p}} K_0(\hat{p}) = \mathscr{L}(\delta) - \mathscr{L}(a_0), \tag{62}$$

$$-\mathscr{L}(\Gamma_c^*)\, e^{-p}\{I_0(p) + I_1(p)\} - (r^2/\pi)\, \mathscr{L}(v^*)\, e^{\hat{p}}\{K_1(\hat{p}) - K_0(\hat{p})\} = \mathscr{L}(a_0) + \mathscr{L}(a_1), \tag{63}$$

where

$$\hat{p} \equiv r^2 p + \epsilon, \tag{64}$$

and I, K are the usual cylinder functions. The functions $\mathscr{L}(a_0)$ and $\mathscr{L}(a_1)$ will be known when the motion of the body is prescribed, while $\mathscr{L}(\Gamma_c^*)$, $\mathscr{L}(v^*)$ and $\mathscr{L}(\delta)$

are three unknown functions. Thus a hypothesis is needed to enable us to close the system.

Let Q be the rate at which the unsteady component of cavity volume is passing into the wake; then $Q = 2U\ \delta y^*$, where $2\delta y^*$ is the unsteady increment to the displacement thickness at S (see figure 11). Now

$$\delta y^* = -\int_{\xi=1}^{\infty} v\,dx, \quad \text{as} \quad \delta y_\infty = 0$$

and $v \approx dy/dx$. Thus

$$Q(\tau) = 2U\,\delta y^*(\tau) = -ULr\int_1^\infty v(\xi, \hat{\tau})\,d\xi,$$

where $\hat{\tau} \equiv \tau/r^2$. Let $V(\tau)$ denote the cavity volume; then conservation of volume requires that $\dot{V} = -Q$. The hypothesis we shall adopt is that a functional relation exists between $\dot{V}(\tau+2)$ and the pressure increment $p_c - p_1 = \rho q^2 F^*(\tau)$. The time

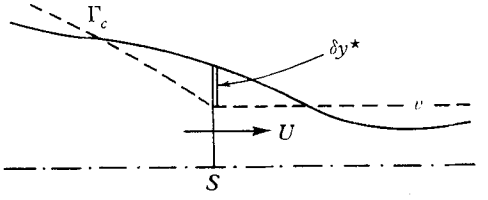

FIGURE 11. Convection of cavity volume.

delay here is introduced on the reasonable assumption that V cannot respond to pressure change immediately, but must wait for the reaction of the re-entrant jet at S to modify the flux of bubbles into the wake, and that in turn the jet strength J can be changed only by the arrival of a wave travelling downstream along the cavity wall. Initially then, on this model, a pressure increase simply modifies the flow direction at separation, and this disturbance is convected along the cavity walls in such a way to keep V constant. Only when this wave reaches S does J change, and then Q can also change.

The problem now is to find the relation between $\dot{V}(\tau+2)$ and $F^*(\tau)$. In view of the complexity of the flow near the re-entrant jet, there seems little chance of doing more than writing down an empirical relationship. The simplest is

$$2ULkF^*(\tau) = \dot{V}(\tau+2) = -Q(\tau+2),$$

where k is an empirical constant. Hence

$$2ULkF^*(\tau) = -Q(\tau+2) = ULr\int_1^\infty v\left(\xi, \frac{\tau+2}{r^2}\right)d\xi, \tag{65}$$

and on transforming this with respect to τ we obtain

$$2k\mathscr{L}(F^*) = \frac{r^3}{r^2 p + \epsilon} e^{2p}\,\mathscr{L}(v^*). \tag{66}$$

Now returning to the question of the additional hypothesis needed to close (62)–(64), we can identify four distinct possibilities:

(i) *A strongly damped wake,* i.e. $v \approx 0$. Large ϵ in (62) requires $v \approx 0$, and so by (66) $k = 0$. We expect this with natural cavities, where the re-absorption of

wake bubbles is rapid. Incidentally if we set $\delta = 0$ and make ϵ large the term containing v^* in (63) vanishes, whereas the corresponding term in (62) contains $v^*/\sqrt{\epsilon}$, and—with v^* large—takes over the role of the singularity. This gives an interpretation of δ rather similar to that shown in figure 8.

Omitting terms involving v^* from (62) and (63), we get

$$\mathscr{L}(\Gamma_c^*) = -\{\mathscr{L}(a_0)+\mathscr{L}(a_1)\}\, e^p/\{I_0(p)+I_1(p)\}, \tag{67}$$

$$\mathscr{L}(\delta) = -\mathscr{L}(a_1)+\{\mathscr{L}(a_0)+\mathscr{L}(a_1)\}\, W(-ip), \tag{68}$$

where

$$W(z) \equiv J_1(z)/\{J_1(z)-iJ_0(z)\}. \tag{69}$$

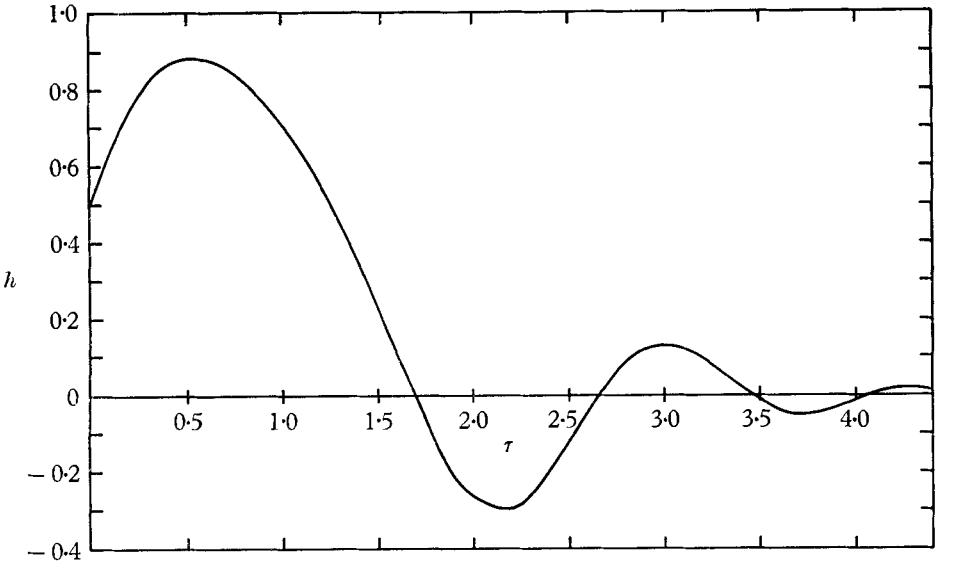

FIGURE 12. The function $h(\tau)$.

Let $h(\tau)$ be the function having $W(-ip)$ as its transform, i.e.

$$h(\tau) \equiv \frac{\mathrm{U}(\tau)}{2\pi i}\int_{c-i\infty}^{c+i\infty} W(-ip)\,\frac{e^{p\tau}}{p}\,dp,$$

then (68) can be inverted to the form

$$\delta = -a_1(\tau)+\int_0^\tau (\dot{a}_0+\dot{a}_1)\,h(\tau-\tau^*)\,d\tau^*, \tag{70}$$

a similar treatment holding for (67). With the notation

$$\begin{bmatrix} c_0 \\ c_1 \end{bmatrix} \equiv \frac{1}{\pi}\int_{-\infty}^{-1} \frac{\Theta}{\sqrt{(\xi^2-1)}} \begin{bmatrix} 1 \\ -\xi \end{bmatrix} d\xi, \tag{71}$$

(56) and (57) can be written for the present case in the forms

$$p_c - p_1 = \rho q_1^2(\delta - a_0 - c_0), \tag{72}$$

$$C_D - C_{D0} = -2\pi(L/c)\,r(\delta + a_1 + c_1). \tag{73}$$

The function $h(\tau)$ is shown in figure 12, and a short table is provided in table 2.

In the light of the discussion of (65) we should expect this theory to hold quite well for all types of cavity for impulsive motions in the time interval $0 < \tau < 2$, before the wave impinges on S and alters the entrainment rate.

(ii) *Constant pressure cavity, i.e.* $F^* \approx 0$. This case ($k = \infty$) requires a high rate of vaporization or, equivalently, a rapid change in the rate of air injection, compared with the rate at which the cavity volume is changing. If we put $r \approx 1$ and $\epsilon \approx 0$, i.e. assume an undamped wake as one may expect with a ventilated cavity, then (72) and (73) also apply here, so $\delta = a_0 + a_1$, and

$$C_D - C_{D0} = -2\pi(L/c)\, r(a_0 + a_1 + c_0 + c_1). \tag{74}$$

(iii) *No singularity, i.e.* $\delta = 0$. This possibility, not contained as a special case of (66), may be worth considering. With an undamped wake (72) and (73), in which δ is now zero, are still applicable. Which of (ii) and (iii) is the more accurate model for times $\tau > 2$ can only be resolved by further experiments.

(iv) *A reacting wake.* In this case an additional physical phenomenon provides a new relation, like (65). For example, the pumping action illustrated in figure 2, which occurs inside rather than outside the cavity, is a phenomenon distinct from the convection of disturbances that forms the physical basis of the theory leading to (62) and (63). This case is discussed in the next section.

7. Resonating cavities

First we note that the above theory can be modified to deal with oscillatory motions of long duration as follows. Let ν be the real frequency in radians per second and define a reduced frequency by $\nu t = \omega\tau$, so that

$$\omega = L\nu/2Ur. \tag{75}$$

Now suppose that $a_0(\tau) = \hat{a}_0 e^{i\nu t} = \hat{a}_0 e^{i\omega\tau}$, $\hat{a}_0$ being a complex amplitude, and that similar expressions for $a_1(\tau)$ and $\Gamma_c^*(\tau)$ are adopted. As v^* is generated at S and must have a phase fixed in relation to the waves incident on S from the cavity, and independent of ω (see discussion of (65)), it is necessary to write

$$v^* = \hat{v}^*\, e^{i\omega(\tau-2)}.$$

Now $\mathscr{L}(a_0) = \hat{a}_0 p/(p - i\omega)$, and the inverses of (62) and (63) are obtained directly on replacing $\mathscr{L}(a_0)$ by $\hat{a}_0$, etc., and p by $i\omega$. For simplicity we take $r \approx 1$ and $\epsilon \approx 0$, and then find from the inverses of (62) and (63) that

$$\hat{v}^* = i\pi\, e^{i\omega}\{(J_0 + iJ_1)(\hat{a}_0 - \hat{\delta}) - J_0(\hat{a}_0 + \hat{a}_1)\}, \tag{76}$$

where the omitted argument of the Bessel functions is ω. Similarly (66) gives

$$k\hat{F}^* = (-i/2\omega)\,\hat{v}^*. \tag{77}$$

Once $\hat{v}^*$ is known the original function can be deduced from (11):

$$v(\xi, \tau) = v(1, \tau - \xi + 1) = \hat{v}^*\, e^{-2i\omega}\, e^{i\omega(\tau-\xi+1)} = \hat{v}^*\, e^{i\omega(\tau-\xi-1)}.$$

Now the experiments described in the introduction show resonance with the body held fixed. In this case a_0 and a_1 are zero, and (76) reduces to

$$\hat{v}^* = \omega\pi\, e^{i\omega}(J_1 - iJ_0)\,\hat{F}^*, \tag{78}$$

as by (56) and (72) it is now the case that $\hat{\delta} = \hat{F}^*$. As k is real in (77), (77) and (78) are compatible only if ω satisfies the equation

$$\sin\omega J_0(\omega) + \cos\omega J_1(\omega) = 0, \tag{79}$$

and if k has the value

$$k = -\pi J_0(\omega)/(2\cos\omega). \tag{80}$$

The first six roots of (79) and the corresponding values of k are shown in table 1. The roots are given closely by $\omega_n = 1{\cdot}97 + \pi(n-1)$. Notice that k is always positive and varies only slowly with ω, in fact like $1/\sqrt{\omega}$. An examination of figure 2 reveals that the physical mechanism there described keeps $p_c - p_1 = \rho q_1^2 F^*$ 90° behind v^*, thus $\hat{F}^* \propto -i\hat{v}^*$, confirming (77).

Experiment	Hydrofoil	ω_n	2·7	5·1	8·2	11·4	14·7	—
	Flat plate	ω_n	2·5	5·0	8·5	11·2	14·1	—
Theory		ω_n	1·97	5·11	8·25	11·39	14·53	17·67
		k_n	0·98	0·57	0·45	0·38	0·33	0·32

TABLE 1. Resonance frequencies

It must be admitted that estimating the length of the cavities from the results given in the paper by Silberman & Song is not easy, and that the good agreement achieved between the present theory and experiment for the resonance frequencies (table 1) may possess some subjective element. Still the error range for the experiments certainly includes the theoretical figure, except possibly for the first-stage cavity. Silberman & Song mention that the convection velocity of cavity waves is rather less than q_1 for some first-stage cavities, so perhaps some discrepancy is to be expected.

A somewhat different explanation of resonating cavities has been given by Song (1962), who concluded by a simple argument that $\omega_n = \pi n$. His treatment, which depends on the presence of outer bounding free surfaces to provide the resonance, treats the flow pattern as equivalent to an oscillating cylindrical gas bubble separated from another gaseous region of infinite extent by an annulus of liquid. The experimental evidence seems insufficient to distinguish the two theories. Free boundaries could be important in *initiating* resonance without in fact being essential to its maintenance.

8. Stability of bodies in cavitating flow

For simplicity we put $\epsilon = 0$ and $r = 1$. Then from (56), (72), (62) and (63) it follows that

$$\mathscr{L}(\delta) = \frac{(2k\,e^{-p}/\pi)\,\mathscr{L}(a_0+c_0) + I_0\,\mathscr{L}(a_1) - I_1\,\mathscr{L}(a_0)}{(2k\,e^{-p}/\pi) - (I_0+I_1)}, \tag{81}$$

where the argument of the cylinder functions is p, and we have made use of the relation $p\{I_0(p)\,K_1(p) + I_1(p)\,K_0(p)\} = 1$. For oscillatory motions we replace $\mathscr{L}(\delta), \mathscr{L}(a_0) \ldots$ by $\hat{\delta}, \hat{a}_0, \ldots$ and p by $i\omega$; then the vanishing of the denominator in (81) is the condition for resonance already studied in § 7. Equations (72) and (73) give $p_c - p_1$ and $C_D - C_{D0}$.

Suppose, for example, a rigid body has a perturbation displacement given by $x = x_2(\tau)$; then, by (9) and (13), $\theta_2 = -\dot{x}_2(2U/L)\sin\theta_0/q_0$. Then from (61) and (71)

$$\left.\begin{aligned}\begin{bmatrix}a_0\\a_1\end{bmatrix} &= -\frac{2}{L}\dot{x}_2\begin{bmatrix}A_0\\A_1\end{bmatrix} = -\frac{2}{L}\hat{x}i\omega\, e^{i\omega\tau}\begin{bmatrix}A_0\\A_1\end{bmatrix},\\ \begin{bmatrix}c_0\\c_1\end{bmatrix} &= -\frac{2}{L}\ddot{x}_2\begin{bmatrix}C_0\\C_1\end{bmatrix} = \frac{2}{L}\hat{x}\omega^2\, e^{i\omega\tau}\begin{bmatrix}C_0\\C_1\end{bmatrix},\end{aligned}\right\} \tag{82}$$

the second form being for oscillatory motions when $x_2 = \hat{x}\,e^{i\omega\tau}$, and where

$$\begin{bmatrix}A_0 & C_0\\A_1 & C_1\end{bmatrix} \equiv \frac{U}{\pi}\int_{\xi_0}^{-1}\frac{\sin\theta_0}{q_0}\begin{bmatrix}1/\sqrt{(\xi^2-1)} & \cosh^{-1}(-\xi)\\ -\xi/\sqrt{(\xi^2-1)} & \sqrt{(\xi^2-1)}\end{bmatrix}d\xi, \tag{83}$$

are numbers depending only on the steady flow. With long cavities the front stagnation point $\xi = \xi_0$ is close to -1, and we find

$$A_0 \approx A_1, \quad C_0 \approx C_1 \approx 0. \tag{84}$$

With oscillatory motions (81) and (82) give

$$\delta = 2\omega\frac{\hat{x}}{L}e^{i\omega\tau}\left\{\frac{2k\,e^{-i\omega}(\omega C_0 - iA_0)/\pi - J_1A_0 + iJ_0A_1}{2k\,e^{-i\omega}/\pi + J_0 + iJ_1}\right\}.$$

Substituting into (73) and adopting the approximation (84), we find that the component of $C_D - C_{D0}$ in phase with the velocity $i\omega\hat{x}\,e^{i\omega\tau}$ is negative only if

$$-(2/\pi)\,k(\cos\omega J_0(\omega) - 2\sin\omega J_1(\omega)\} > (2k/\pi)^2 + \{J_1(\omega)\}^2. \tag{85}$$

This is the condition for stability of the body, and it does not appear that it can be satisfied for positive values of k.

τ	h	τ	h	τ	h	τ	h	τ	h
0·0	0·500	1·4	0·353	2·8	0·087	4·2	0·015	6·5	0·001
0·2	0·734	1·6	0·117	3·0	0·139	4·4	0·016	7·0	0·011
0·4	0·868	1·8	−0·112	3·2	0·098	4·6	−0·005	7·5	−0·016
0·6	0·889	2·0	−0·268	3·4	0·022	4·8	−0·024	8·0	0·015
0·8	0·826	2·2	−0·298	3·6	−0·034	5·0	−0·021	8·5	−0·009
1·0	0·710	2·4	−0·204	3·8	−0·040	5·5	0·028	9·0	0·000
1·2	0·554	2·6	−0·047	4·0	−0·012	6·0	−0·016		

TABLE 2. The function $h(\tau)$

9. Growth of drag due to a sudden change in velocity

If attention is confined to the time interval $\tau < 2$, then it is reasonable to assume that $v = 0$—see discussion in § 6. Then with $(2Ur/L)\dot{x}_2 = -V\mathbf{U}(\tau)$, so that the new upstream velocity becomes $(U+V)$, we find

$$\begin{bmatrix}a_0\\a_1\end{bmatrix} = \frac{V}{q_1}\begin{bmatrix}A_0\\A_1\end{bmatrix}\mathbf{U}(\tau).$$

Then by (70), (72) and (73)

$$p_c - p_1 = \rho q_1 V(A_0 + A_1)\{h(\tau) - \mathbf{U}(\tau)\}, \tag{86}$$

$$C_D - C_{D0} = -2\pi(LV/cU)(A_0 + A_1)h(\tau), \tag{87}$$

which can be plotted with the aid of figure 12. For long cavities and slender bodies it follows from (45) that $(A_0+A_1) \approx 4m\theta_a/\pi$.

It must be remembered that these results can be used only if $\tau < 2$. At longer times the cavity changes its volume and the pressure and forces tend to the values appropriate to the new upstream velocity $(U+V)$.

REFERENCES

BENJAMIN, T. B. 1964 *J. Fluid Mech.* **19**, 137.

SILBERMAN, E. & SONG, C. S. 1961 *J. Ship Res.* **5**, no. 1, 13–33.

SONG, C. S. 1962 *J. Ship Res.* **5**, no. 4, 8–20.

VAN DER POL, B. & BREMMER, H. 1950 *Operational Calculus Based on the Two-sided Laplace Integral.* Cambridge University Press.

WOODS, L. C. 1961 *The Theory of Subsonic Plane Flow.* Cambridge University Press.

WOODS, L. C. 1964 *J. Fluid Mech.* **19**, 124–136.